PROTEIN ENGINEERING

Volume 11 number 6 June 1998

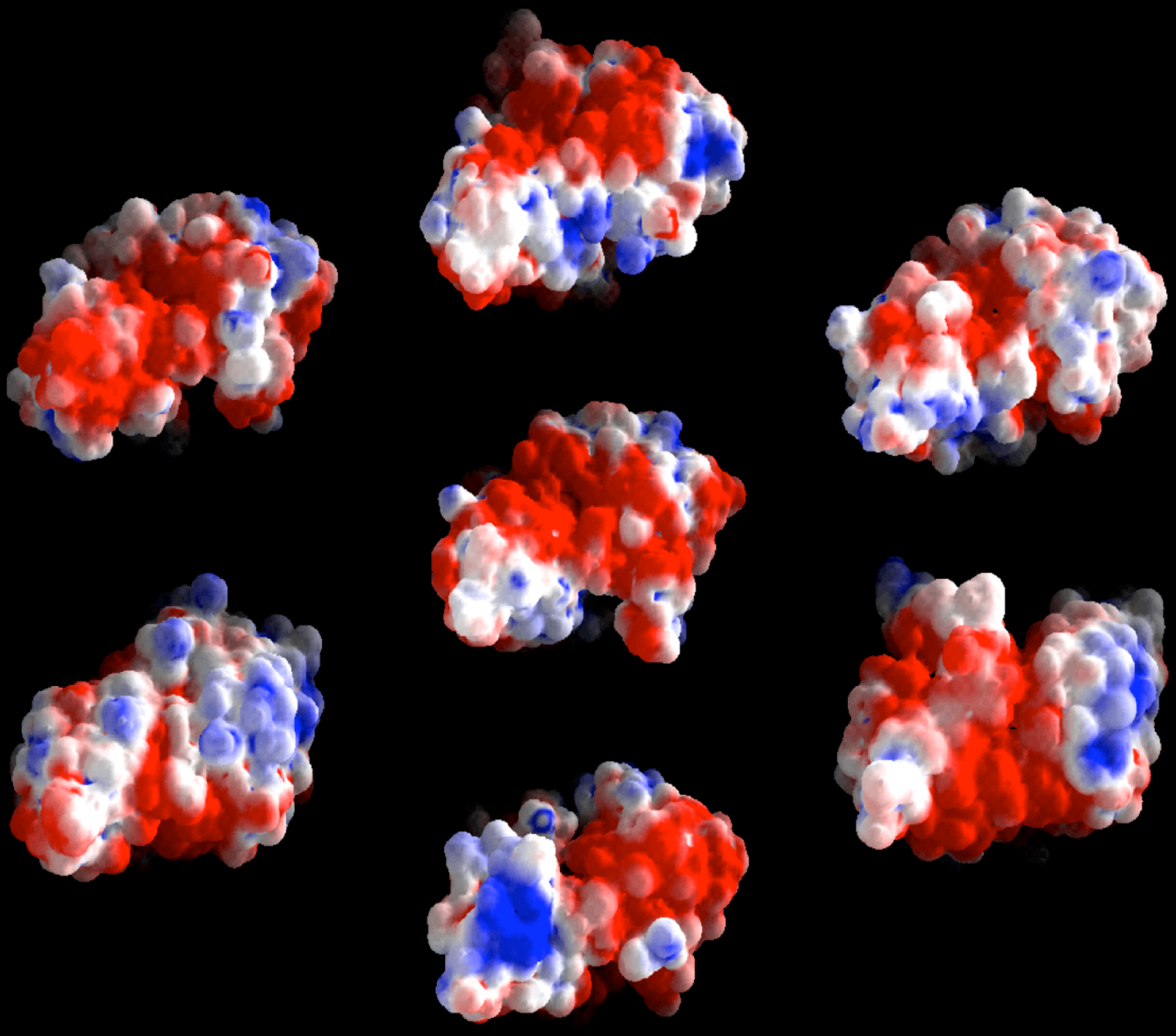

Electrotactins: molecular recognition via electrostatic motifs

Protein Engineering vol.11 no.6 pp.415–420, 1998

Electrotactins: a class of adhesion proteins with conserved electrostatic and structural motifs

Simone A.Botti[1,2], Clifford E.Felder[2], Joel L.Sussman[2,3,4] and Israel Silman[1]

Departments of [1]Neurobiology and of [2]Structural Biology, Weizmann Institute of Science, 76100 Rehovot, Israel and [3]Biology Department, Brookhaven National Laboratory, Upton NY 11973, USA

[4]To whom correspondence should be addressed

The concept of an electrostatic motif on the surface of biological macromolecules as a definite topographical pattern of electrostatic potentials in three-dimensional space, provides a powerful tool for identification of functionally important regions on the surface of structurally related macromolecules. Using this approach, we identify a functional region common to cholinesterases (ChEs) and to a set of neural cell-adhesion proteins that have been suggested to be structurally related to cholinesterases due to their high sequence similarity, but lacking the key catalytically active serine. Quantitative analysis of the electrostatic surface potential in the area surrounding the entrance to the active site of acetylcholinesterase, and in the analogous zone for the ChE-like domain of the adhesion proteins reveals very good correlation. These findings, examined in the context of previous evidence involving this same region in a possible cell-recognition function for ChEs, leads us to define a class of adhesion proteins which we have named 'electrotactins'.

Keywords: acetylcholinesterase/cell adhesion/electrostatics/nervous system/homology modelling

The concept of an electrostatic motif on the surface of biological macromolecules as a definite topographical pattern of electrostatic potentials in three-dimensional space (3D), provides a powerful tool for identification of functionally important regions on the surface of structurally related macromolecules (Honig and Nicholls, 1995). This pattern can only be defined in the context of molecules of similar 3D structure, for only in such a case is it possible to unambiguously orient the motif with respect to zones of the related macromolecules which might be functionally significant. We use this approach to localize a functional region common to cholinesterases (ChEs), a family of enzymes of the nervous system, and to a set of neural cell-adhesion proteins, which includes gliotactin (GLI), neurotactin (NRT) and neuroligin (NL), that have been suggested to be structurally related to ChEs due to their high sequence similarity (Krejci *et al.*, 1991), but lack the catalytically active serine. This enables us to identify structural properties involved in possible cell-adhesion functions of ChEs.

Cholinesterases are a family of enzymes which fall broadly into two types, acetylcholinesterase (AChE) and butyrylcholinesterase (BChE). They are distinguished primarily by their substrate specificity: AChE hydrolyzes acetylcholine (ACh) faster than other choline esters and is much less active on butyrylcholine, whereas BChE displays similar activity towards the two substrates (Mendel and Rudney, 1943; Chatonnet and Lockridge, 1989). Although the main physiological function of AChE is believed to be termination of impulse transmission at cholinergic synapses by rapid hydrolysis of ACh, the function of BChE is still unknown. The 3D structure of AChE has been solved (Sussman *et al.*, 1991), and the high degree of identity among AChE and BChE sequences has permitted construction of homology models of the 3D structures of BChE (Harel *et al.*, 1992) and of AChE from different species. Inspection of these structures has shown that the active site of the ChEs is located at the bottom of a deep and narrow gorge. Examination of the 3D structure of *Torpedo californica* AChE (*Tc*AChE) showed the enzyme to be characterized by a marked asymmetric spatial distribution of charged residues, that were shown to roughly segregate into a 'northern' negative hemisphere (taking the mouth of the gorge as the north pole) and a 'southern' positive one (Ripoll *et al.*, 1993). This electrostatic pattern was shown to give rise to a large dipole moment which was calculated to be ~1600 Debye and roughly oriented along the axis of the active-site gorge (Ripoll *et al.*, 1993; Tan *et al.*, 1993; Antosiewicz *et al.*, 1994). Electro-optical measures performed on AChE from *Bungarus fasciatus* gave a value of ~1000 Debye, thus confirming experimentally the order of magnitude of the macrodipole (Porschke *et al.*, 1996).

The asymmetric distribution of surface potentials was thought to be essential for the fast catalysis effected by ChEs. This assumption has been reevaluated in the light of site-directed mutagenesis experiments on human AChe (hAChE) in which up to seven charged residues in the vicinity of the entrance to the active-site gorge were neutralized. The ensuing drastic reduction of the asymmetric distribution of surface potentials did not have a major effect on catalysis (Shafferman *et al.*, 1994). Brownian dynamics simulations of bimolecular rate association constants for ACh and AChE also failed to show a meaningful correlation between the distribution of electrostatic surface potentials and catalysis (Antosiewicz *et al.*, 1996). A further analysis of the electrostatic properties of the 3D structures and homology models of ChEs, aimed at generating a detailed and quantitative topographical map of the electrostatic surface potentials, identified the presence of an 'annular' electrostatic motif of negative surface potential around the entrance of the active site gorge (Felder *et al.*, 1998). The role of surface potentials in catalysis is not clear-cut. It has been shown to play only a minor role in the case of isozymes of trypsin differing by as much as 12.5 charge units. The catalytic efficiency of these isozymes was shown to be influenced not by electrostatic surface potentials, but by a few charged amino acids localized close to the active site. (Soman *et al.*, 1989). These considerations drove us to investigate whether the role of surface potentials in ChE might be related to roles other than catalysis.

ChEs possess a 3D fold different from those of 'classical' serine-hydrolases, such as chymotrypsin or subtilisin. This fold is called the α/β hydrolase fold (Ollis *et al.*, 1992)

and has been shown to characterize a family of hydrolytic enzymes of widely different phylogenetic origin and substrate specificity. Some of these enzymes, like the fungal triacylglycerol lipases from *Geotrichum candidum* and *Candida rugosa* (Cygler *et al.*, 1993), show substantial sequence similarity with ChEs. Other members of the family, like haloalkane halogenase from *Xenobacter autotrophicus* and dienelactone hydrolase from *Pseudomonas* sp., do not show significant sequence similarity to the ChEs; but inspection of their 3D structures shows that their polypeptide chain has the structural core typical of the α/β hydrolase fold (Ollis *et al.*, 1992). A systematic search of sequence databases has retrieved a large number of proteins with a high degree of sequence similarity to α/β hydrolases (Krejci *et al.*, 1991). Inspection of the sequences reveals that amongst an overwhelming majority of enzymes, there are also a few proteins involved in cell adhesion; these contain a ChE-like domain whose function is most probably independent of hydrolase activity since the active-site serine is mutated to a glycine. Amongst them are the three proteins which we chose to investigate, because of their presumed involvement in cell adhesion and signaling in the nervous system.

GLI is a transmembrane protein transiently expressed on peripheral glia of *Drosophila melanogaster* embryos and required for formation of the peripheral blood–nerve barrier (Auld *et al.*, 1995). The C-terminal extracellular domain of this protein shows substantial sequence similarity with ChEs. Such similarity can also be found in the extracellular domain of NRT, a transmembrane glycoprotein which is expressed in neuronal and epithelial tissues during embryonic and larval stages (Barthalay *et al.*, 1990; Hortsch *et al.*, 1990). Sequence similarities suggest that neuroligins (NLs), a family of mammalian neuronal cell surface proteins that act as ligands for β-neurexins (Ichtchenko *et al.*, 1995), also contain an extracellular ChE-like domain. NLs and neurexins mediate interactions between neurons and contribute to the specific organization of synapses. All these proteins are involved in heterophilic cell–cell interactions, suggesting that their ChE-like domains possess a recognition function that has been conserved from invertebrates to vertebrates. It is worth noticing that both GLI and NRT display substantially higher sequence similarity with *Tc*AChE than with the *D.melanogaster* enzyme (*Dm*AChE) (Table I) and that the targets of their adhesive functions have not yet been identified.

The sequence similarity between ChEs, NL, GLI and NRT prompted us to build homology models of their extracellular domains, both to confirm the presence of shared structural motifs and to investigate the possibility that they might display similar electrostatic characteristics. Our underlying assumption is that the ChE-like domains of these adhesion proteins are independently folded, and that neither their conformation nor their electrostatic properties will be greatly affected by the association with the non-ChE like regions of GLI, NL and NRT, which are mostly transmembrane and intracellular (Figure 1).

The homology models were built with the automated knowledge-based building tool Swiss-Model (Peitsch, 1995) and validated as described previously (Felder *et al.*, 1998). The same modeling procedure was applied as a control to the neutral lipase from *G.candidum* (*Gc*Lip) (Schrag and Cygler, 1993) whose 3D structure is known, to check for the bias in modeling introduced by the templates. The modeling of *Gc*Lip gave a structure very close to the actual 3D structure solved by X-ray crystallography (α-carbon r.m.s. deviation ~1.1 Å from the 3D X-ray structure of *Gc*Lip). Since all the proteins involved in this study possess about the same degree of sequence identity as *Gc*Lip does with *Tc*AChE (Table I), we can reasonably assume our models to be close approximations of the actual structures of these domains.

Table I. Percent sequence identity and similarity between electrotactins, lipases and ChEs as given by the BestFit algorithm from the GCG package (version 9, Genetics Computer Group, 575 Science Drive, Madison, WI 53711, USA)

Protein	Percent identity to *Tc*AChE (*DmAChE)*	Percent similarity to *Tc*AChE (*DmAChE*)
Cholinesterases		
*Tc*AChE	100.0	100.0
hAChE	57.6	85.0
mAChE	59.0	85.3
*Dm*AChE	36.3	65.8
7-hAChE	57.6	85.0
hBChE	52.4	83.1
Adhesion proteins		
NRT (*Dros.*)	31.1 (*25.1*)	57.7 (*50.4*)
GLI (*Dros.*)	30.6 (*23.5*)	61.0 (*55.7*)
NL (mouse)	32.3	60.1
Lipases		
*Gc*Lip	29.4	56.8
rBSSL	31.2	61.4
*Cr*CE	31.9	56.8

The values are calculated with respect to the sequence of *Tc*AChE.

The electrostatic surface potentials of *Tc*AChE (PDB entry 2ACE), GLI, NL and NRT were calculated solving the Poisson–Boltzmann equation by the finite difference method (FDPB) (Warwicker and Watson, 1982), using the DelPhi algorithm (Gilson and Honig, 1988) as implemented in the GRASP program (Nicholis *et al.*, 1991). As a control, we checked the distribution of surface potentials for other members of the α/β hydrolase family to check whether the 'annular' electrostatic motif was a characteristic shared by most members of this family. We chose three enzymes with a sequence identity to ChEs similar to that of NL, NRT and GLI. The three enzymes selected were cholesterol esterase from *Candida rugosa* (Ghosh *et al.*, 1995) (*Cr*CE, PDB entry 1CLE), *Gc*Lip (PDB entry 1THG) and bile-salt-stimulated lipase from rat (rBSSL) (Kissel *et al.*, 1989). In this last case the 3D structure is not yet available, and a homology model was built following the same procedure used for GLI, NRT and NL. We also calculated the surface potentials for wild-type human BChE (hBChE), for human AChE (hAChE) and for the mutant of hAChE in which seven negatively charged residues near the entrance of the gorge had been neutralized (7-hAChE). The structures of 7-hAChE, NL, NRT GLI, *Gc*Lip, *Cr*CE and rBSSL were superimposed on that of *Tc*AChE by a least-squares fitting procedure implemented in the program LSQMAN (Kleywegt, 1996), and placed in a common orientation in which the axis of the active-site gorge of *Tc*AChE (as defined by Antosiewicz *et al.*, 1994) is aligned with the cartesian Z-axis.

Our most significant result is shown in Figure 2. It is immediately apparent that the electrostatic surface potential contours of *Tc*AChE, GLI, NRT and NL are strikingly similar. All three proteins show a characteristic 'annular' electrostatic motif of negative potential around the zone homologous to the active-site gorge of the ChEs. In contrast, *Gc*Lip, rBSSL and

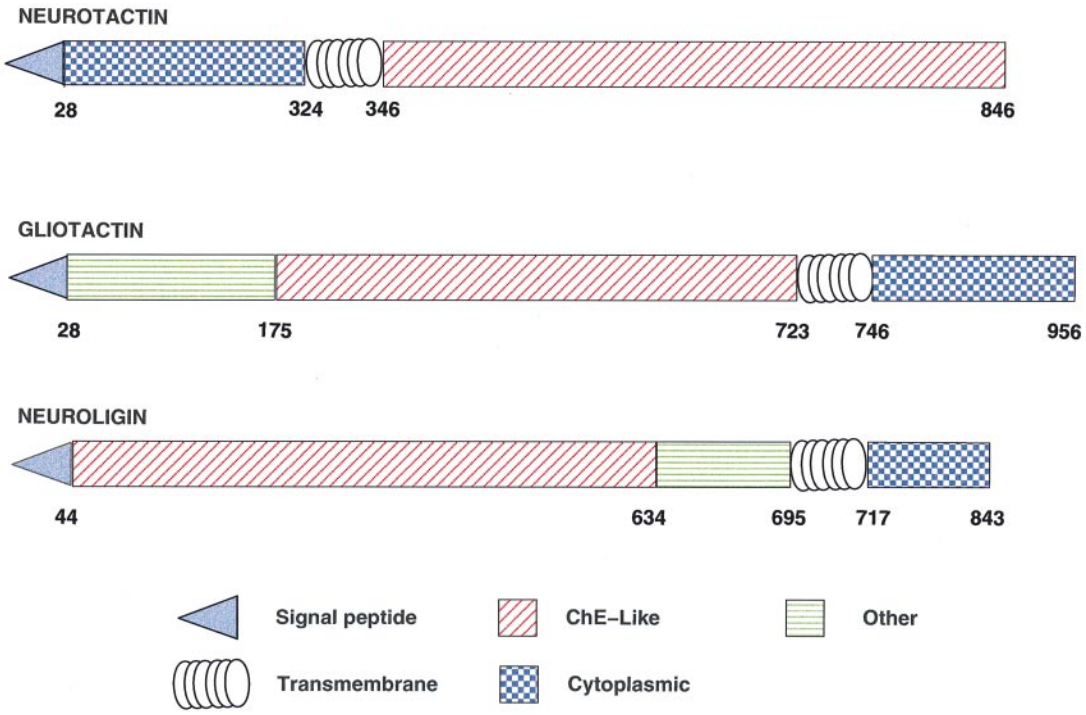

Fig. 1. Schematic representations of the domain organizations of GLI, NRT and NL.

*Cr*CE appear to display a different topographical distribution of surface potentials (Figure 2a).

In the case of the 7-hAChE mutant, neutralization of seven negatively charged residues in the 'annular' region virtually erases the electrostatic motif, while not affecting the negative potential gradient within the active-site gorge. This distribution of electrostatic surface potentials is very similar to that of hBChE (Figure 2b). This finding correlates well with the contention that the potential gradient inside the active-site gorge makes a more important contribution to ChE catalysis than the surface potentials around the rim of the active-site gorge (Shafferman *et al.*, 1994; Zhou *et al.*, 1996).

In order to provide a quantitative measure of the electrostatic motif of the molecules studied, we calculated the average surface potential over a 20 Å wide region of accessible surface around the zone homologous to the entrance of the active site gorge of *Tc*AChE (which constitutes the common Z axis). This region was divided into 1 Å wide concentric sections, and the average potentials in the sections were plotted and correlated by a linear regression fit with the results obtained for *Tc*AChE (Table II and Figure 3). GLI, NRT and NL are all characterized by a high correlation coefficient and an average potential in the 'annular' region very similar to that of *Tc*AChE; in addition, their potential gradient closely follows that of *Tc*AChE. Of the three lipases, only *Cr*CE shows a high correlation coefficient and an average potential similar to AChE, but its r.m.s. deviation from the ChE-like fold is the largest amongst all the proteins examined, and its potential gradient is substantially different from that of *Tc*AChE. It is of interest that hBChE displays a lower average potential in the 'annular' region and a very poor correlation coefficient, in addition to a potential gradient similar to that of the lipases.

The biological significance of the electrostatic surface potential of ChEs has been the subject of speculations, and it has been proposed that it might have a non-catalytic function (Shafferman *et al.*, 1994). There is mounting evidence that ChEs may be involved in functions distinct from their catalytic activity. During development of the nervous system of vertebrates, expression of ChEs is associated with periods of enhanced neurite outgrowth (Layer and Willbold, 1994; Layer *et al.*, 1993), suggesting that they might serve as neuronal growth factors or cell-adhesion molecules. It has been speculated that the site responsible for the non-catalytic interaction of ChEs is localized close to the entrance of the active-site gorge, perhaps overlapping with what has been termed the 'peripheral' anionic site (PAS) of AChE, a possible locus of regulation of enzymatic activity (Radic *et al.*, 1991; Eichler *et al.*, 1994; Barak *et al.*, 1995), which is located in the region of the 'annular' electrostatic motif. In a recent study, AChE was shown to promote neurite regeneration in cultured adult neurons of the mollusk *Aplysia* (Srivatsan and Peretz, 1997). The growth-promoting action of AChE was shown to be independent of its catalytic function. Inhibition of the active site did not influence the neurotrophic action of AChE, but occupancy of its PAS suppressed neurite regeneration (Srivatsan and Peretz, 1997). There is also evidence that the PAS of AChE can enhance the rate of formation of amyloid fibrils, a major component of the senile plaques found in the brains of Alzheimer patients (Inestrosa *et al.*, 1996). Strong evidence for a common recognition mechanism in cell-adhesion between ChEs, GLI and NLs comes from a recent study, in which chimeric constructs of the C-terminal transmembrane domain of NRT, fused to the extracellular cholinesterase-like domains of *Dm*AChE or *Tc*AChE, were shown to be endowed with the same heterophilic adhesion properties as wild type NRT (Darboux *et al.*, 1996).

Electrostatic complementarity between interacting proteins has been found to be one of the major driving forces for complex formation (McCoy *et al.*, 1997). Mutagenesis and electrostatic screening studies of the association rates between barnase, a ribonuclease, and barstar, its inhibitor, have shown the limiting step to be the formation of a binding transition

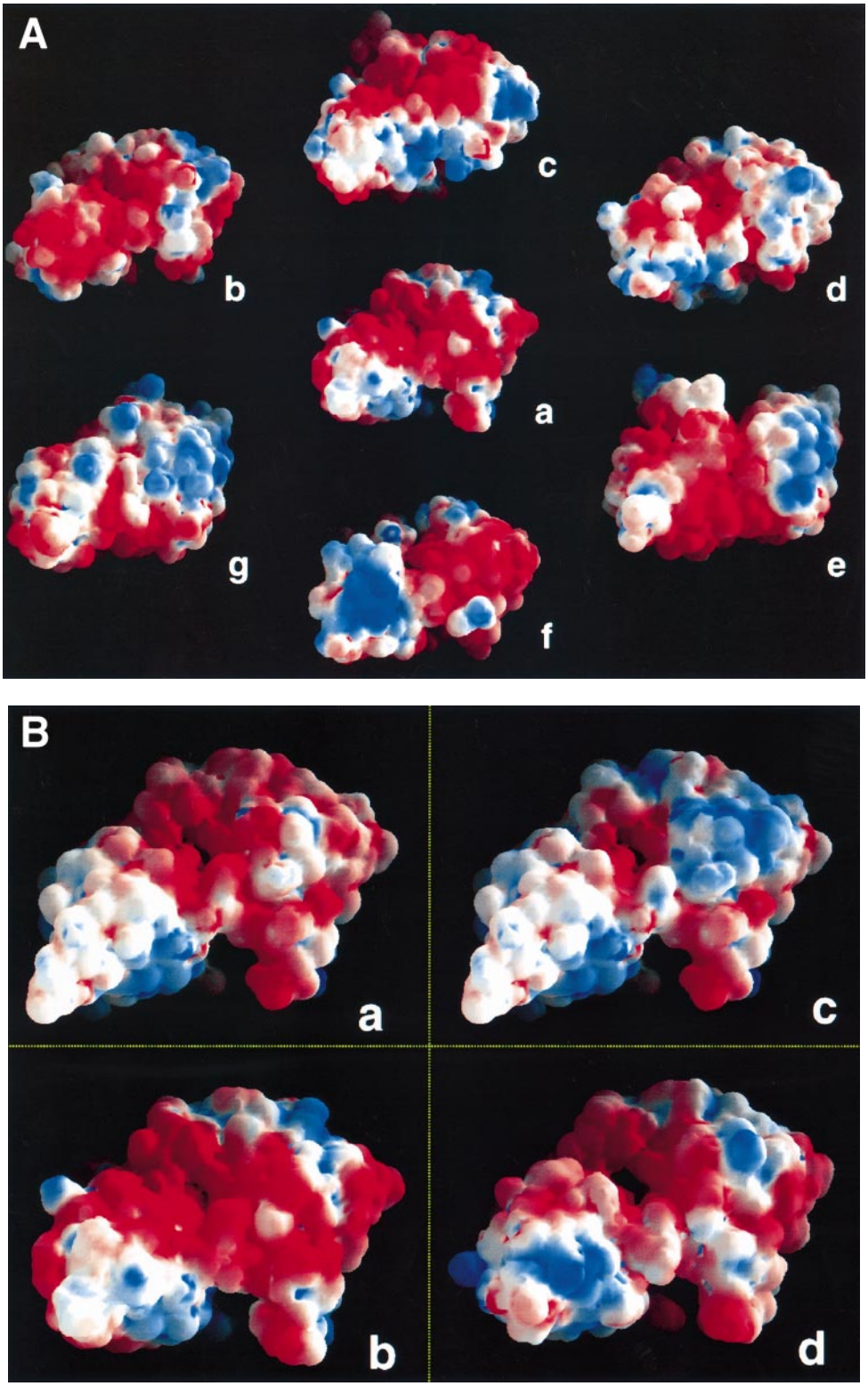

Fig. 2. (**a**) GRASP representations of the distribution of electrostatic surfaces potentials for (a) *Tc*AChE; (b) NRT; (c) NL; (d) GLI; (e) *Cr*CE; (f) rBSSL; (g) *Gc*Lip, showing the presence of the 'annular' electrostatic motif in the adhesion molecules and AChE. The values of surface potentials are expressed as a spectrum ranging from $+0.25kT/e$ (deep blue) through 0 kT/e (white) to -0.25 kT/e (deep red). At a temperature of 298.15 K, $kT/e = 25.7$ mV. The surface potentials are calculated for a salt concentration of 0.145 M, with a cubic grid of linear dimensions of 65 Å, a protein dielectric constant of 4 and a solvent dielectric constant of 78. (**b**) GRASP representations of the distribution of electrostatic surface potentials for (a) hAChE; (b) *Tc*AChE; (c) 7-hAChE and (d) hBChE, showing the absence of the 'annular' motif in hBChE and its neutralization in the 7-hAChE mutant. Calculation and color coding of surface potential values are the same as for Figure 2a.

Table II. R.m.s. structural deviation (Å) of the Cα atoms, average surface potentials (*kT*/*e*) and correlation coefficients for electrostatic surface potentials between electrotactins, lipases and ChEs

Protein	R.m.s. deviation (Å) of Cα atoms relative to *Tc*AChE (percent of matched residues)	Average surface potentials (*kT*/*e*) in the 'annular' motif region	Correlation coefficients for surface potentials in concentric sections of the 'annular' motif region
Cholinesterases			
*Tc*AChE	0.00 (100)	**−2.272**	**1.00**
hAChE	0.48 (97.9)	**−1.139**	**0.89**
mAChE	0.31 (97.1)	**−1.409**	**0.80**
*Dm*AChE	0.77 (98.1)	**−2.358**	**0.86**
7-hAChE	0.48 (97.9)	−0.052	0.90
hBChE	0.42 (94.9)	−0.724	0.66
Adhesion proteins			
Nrt (*Dros.*)	1.19 (94.7)	**−2.132**	**0.83**
Gli (*Dros.*)	1.12 (86.5)	**−1.194**	**0.94**
NL-1 (mouse)	1.10 (84.6)	**−1.332**	**0.89**
Lipases			
*Gc*Lip	1.46 (64.4)	−0.551	−0.45
rBSSL	0.85 (93.0)	−0.020	0.59
*Cc*Lip	1.54 (71.5)	−1.571	0.89

The values are calculated with respect to the 3D structure and electrostatic properties of *Tc*AChE.

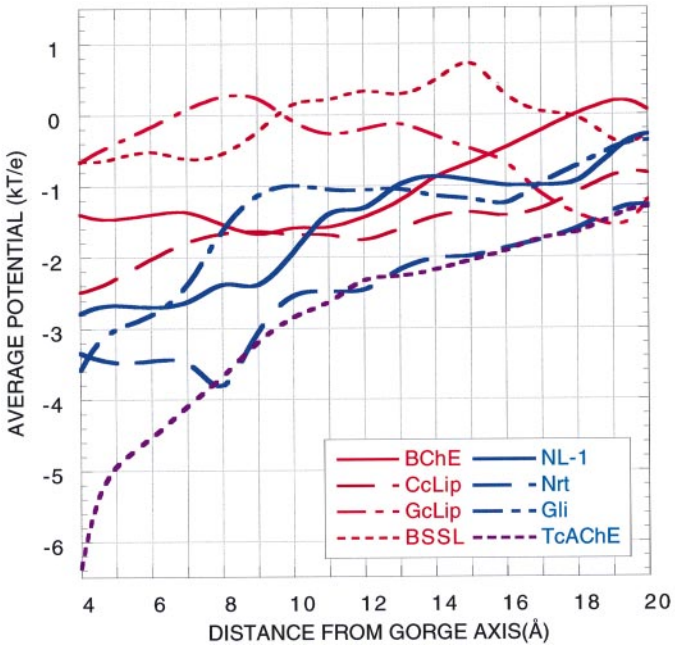

Fig. 3. Plots of average surface potentials measured in concentric sections of the 'annular' motif region for hBChE, *Cr*Ce, *Gc*Lip, BSSL, NL, NRT, GLI and *Tc*AChE. The origin is placed on the axis of the active-site gorge of *Tc*ChE (Antosiewicz *et al.*, 1994) and the potential values are expressed in units of *kT*/*e*, where *k* is Boltzmann's constant, *T* the temperature in *K* and *e* the electronic charge. At a temperature of 298. 15 K, *kT*/*e* = 25.7 mV.

state, in which the two proteins form a low-affinity non-specific complex held together by long-range electrostatic interactions (Schreiber and Fersht, 1996). We speculate that a possible mechanism effected by the 'annular' motif might be the facilitation of target recognition via low specificity associations mediated by long-range electrostatic interactions with a pool of ligands displaying a complementary motif, followed by a subsequent docking step with the unique functional ligand(s), to yield the final high affinity complex. Some support for our hypothesis comes from the mode of binding of AChE to one of its strongest inhibitors, fasciculin II (FAS), a three-fingered polypeptide toxin from the venom of the green mamba (Karlsson *et al.*, 1984). These polypeptide snake venom toxins constitute a family of 6–8 kDa proteins, of which α-bungarotoxin, a potent antagonist for the nicotinic ACh receptor, is the best known member.

FAS has been shown to bind in a 'cork-and-bottle fashion' to the entrance of the active-site gorge of AChE which is situated in the negatively charged 'northern' hemisphere (Bourne *et al.*, 1995; Harel *et al.*, 1995). The surface complementarity between enzyme and inhibitor is very large; about 2000 Å^2 of accessible surface are buried upon binding, including the region of the 'annular' motif. In addition to this large surface complementarity, the AChE–FAS complex displays significant electrostatic complementarity. Analysis of the topography of surface potentials of FAS shows that it also possesses a 'bipolar' motif, with a preponderance of positive surface which is absent in other three-fingered snake toxins. (Karlsson *et al.*, 1984). This positive surface characterizes the zone of interaction between FAS and AChE (Harel *et al.*, 1995).

Analysis of the sequence alignment of the proteins we investigated shows no sequence motif shared exclusively by AChE, GLI, NRT and NL. Thus the conjunction of the topographical distribution of surface potentials with the topological arrangement of the polypeptide chain seems the most important common structural factor conserved between these proteins. It is thus plausible that the shared electrostatic motif indicates a common recognition mechanism or even a common ligand. We hypothesize that a chimeric construct of the cytoplasmic domain of NRT with the mutant form of AChE, in which seven negative residues have been neutralized to abolish the electrostatic motif, will not display the same adhesive properties as a construct built with wild-type AChE. We further predict that constructs with hBChE and *Cr*CE will not be able to promote heterogeneous cell adhesion, the former because it lacks the 'annular' motif, and the latter because of a large deviation from the common ChE-like fold.

The above considerations lead us to conclude that GLI, NRT, NLs and AChE are the first members of a class of adhesion proteins that, because of their common electrostatic and structural motif, we have named 'electrotactins'.

Acknowledgements

The authors wish to thank Gitay Kryger, Charles Millard and Mia Raves for valuable discussions, and Kurt Giles, Amnon Horowitz and Gideon Schreiber for their critical comments on the manuscript. This work was supported by the US Army Medical Research Acquisition activity under Contract no. 17-97-2-7022, the Kimmelman Center for Biomolecular Structure and Assembly, Rehovot, Israel, and the European Union. I.S. is Bernstein-Mason Professor of Neurochemistry. The generous support of Mrs Tania Friedman is gratefully acknowledged.

References

Antosiewicz,J., Gilson,M.K. and McCammon,A. (1994) *Israel J. Chem.*, **34**, 151–158.

Antosiewicz,J., Wlodek,S.T. and McCammon,J.A. (1996) *Biopolymers*, **39**, 85–94.

Auld,V.J., Fetter,R.D., Broadie,K. and Goodman,C.S. (1995) *Cell*, **81**, 757–767.

Barak,D. *et al.* (1995) *Biochemistry*, **34**, 15444–15452.

Barthalay,Y., Hipeau-Jacquotte,R., de la Escalera,S., Jimenez,F. and Piovant,M. (1990) *EMBO J.*, **9**, 3603–3609.

Bourne,Y., Taylor,P. and Marchot,P. (1995) *Cell*, **83**, 503–512.

Chatonnet,A. and Lockridge,O. (1989) *Biochem. J.*, **260**, 625–634.

Cygler,M., *et al.* (1993) *Protein Sci.*, **2**, 366–382.

Darboux,I., Barthalay,Y., Piovant,M. and Hipeau-Jacquotte,R. (1996) *EMBO J.*, **15**, 4835–4843.

Eichler,J., Anselment,A., Sussman,J.L., Massoulíe,J. and Silman,I. (1994) *Mol. Pharmacol.*, **45**, 335–340.

Felder,C.E., Botti,S.A., Lifson,S., Silman,I. and Sussman,J.L. (1997) J. Mol. Graphics Mod., **15**, 318–327.

Ghosh,D. *et al.* (1995) *Structure*, **3**, 279–288.

Gilson,M.K. and Honig,B. (1988) *Proteins*, **4**, 7–18.

Harel,M. *et al.* (1992) *Proc. Natl Acad. Sci. USA*, **89**, 10827–10831.

Harel,M., Kleywegt,G.J., Ravelli,R.B.G., Silman,I. and Sussman,J.L. (1995) *Structure*, **3**, 1355–1366.

Honig,B.H. and Nicholls,A. (1995) *Science*, **268**, 1144–1149.

Hortsch,M., Patel,N.H., Bieber,A.J., Traquina,Z.R. and Goodman,C.S. (1990) *Development*, **110**, 1327–1340.

Ichtchenko,K. *et al.* (1995) *Cell*, **81**, 435–443.

Inestrosa,N.C. *et al.* (1996) *Neuron*, **16**, 881–891.

Karlsson,E., Mbugua,P.M. and Rodriguez-Ithurralde,D. (1984) *J. Physiol.* (Paris), **79**, 232–240.

Kissel,J.A., Fontaine,R.N., Turck,C.W., Brockman,H.L. and Hui,D.Y. (1989) *Biochim. Biophys. Acta.*, **1006**, 227–236.

Kleywegt,G.J. LSQMAN, version 960821/4.7.3. For the Department of Molecular Biology, University of Uppsala, Uppsala, Sweden, 1996.

Krejci,E., Duval,N., Chatonnet,A., Vincens,P. and Massoulíe,J. (1991) *Proc. Natl Acad. Sci. USA*, **88**, 6647–6651.

Layer,P.G., Weikert,T. and Alber,R. (1993) *Cell Tissue Res.*, **273**, 219–226.

Layer,P.G. and Willbold,E. (1994) *Int. Rev. Cytol.*, **151**, 139–181.

McCoy,A.J., Epa,V.C. and Colman,P.M. (1997) *J. Mol. Biol.*, **268**, 570–584.

Mendel,B. and Rudney,H. (1943) *Biochem. J.*, **37**, 59–63.

Nicholls,A., Sharp,K. and Honig,B. (1991) *Proteins: Struct. Funct. Genet.*, **11**, 281–296.

Ollis,D.L. *et al.* (1992) *Protein Engng*, **5**, 197–211.

Pietsch,M.C. (1995) *Bio/Technology*, **13**, 658–660.

Porschke,D. *et al.* (1996) *Biophys. J.*, **70**, 1603–1608.

Radic,Z., Reiner,E. and Taylor,P. (1991) *Mol. Pharmacol.*, **39**, 98–104.

Ripoll,D.R., Faerman,C.H., Axelsen,P.H., Silman,I. and Sussman,J.L. (1993) *Proc. Natl Acad. Sci. USA*, **90**, 5128–5132.

Schrag,J.D. and Cygler,M. (1993) *J. Mol. Biol.*, **230**, 575–591.

Schreiber,G. and Fersht,A.R. (1996) *Nature Struct. Biol.*, **3**, 427–431.

Shafferman,A. *et al.* (1994) *EMBO J.*, **13**, 3448–3455.

Soman,K., Yang,A.S., Honig,B. and Fletterick,R. (1989) *Biochemistry*, **28**, 9918–9926.

Srivatsan,M. and Peretz,B. (1997) *Neuroscience*, **77**, 921–931.

Sussman,J.L. *et al.* (1991) *Science*, **253**, 872–879.

Tan,R.C., Truong,T.N., McCammon,J.A. and Sussman,J.L. (1993) *Biochemistry*, **32**, 401–403.

Warwicker,J. and Watson,H.C. (1982) *J. Mol. Biol.*, **157**, 671–679.

Zhou,H.X., Briggs,J.M. and McCammon,J.A. (1996) *J. Amer. Chem. Soc.*, **118**, 13069–13070.